Langmuir

Article

pubs.acs.org/Langmuir

Salt-Induced Control of Supramolecular Order in Biocatalytic Hydrogelation

Sangita Roy,*[,†] Nadeem Javid,[†] Jan Sefcik,[‡] Peter J. Halling,[†] and Rein V. Ulijn*[,†]

[†]WestCHEM/Department of Pure and Applied Chemistry, University of Strathclyde, 295 Cathedral Street, Glasgow, G1 1XL, United Kingdom

[‡]Department of Chemical and Process Engineering, University of Strathclyde, 75 Montrose Street, Glasgow G1 1XJ, United Kingdom

Supporting Information

ABSTRACT: Biocatalytic action and specific ion effects are both known to have dramatic effects on molecular self-assembly and hydrogelation. In this paper, we demonstrate that these effects are highly cooperative. Biocatalytic hydrogelation of Fmoc peptides in the presence of salts combines kinetic (through enzymatic catalysis) and thermodynamic (specific ion and protein templating) contributions when applied in combination. Spectroscopic data (obtained by fluorescence spectroscopy and circular dichroism) revealed that hydrophobic interactions are greatly affected, giving rise to differential chiral organization and supramolecular structure formation. The kinetic effects of catalytic action could be removed from the system by applying a heat/cool cycle, giving insight into the thermodynamic influence of both protein and salt on these systems and showing that the effects of catalysis, templating, and salts are cooperative. The variable molecular interactions are expressed as variable material properties, such as thermal stability and mechanical strength of the final gel-phase material. To gain more insight into the role of the enzyme, beyond catalysis, in the underlying mechanism, static light scattering is performed, which indicates the different mode of aggregation of the enzyme molecules in the presence of different salts in aqueous solution that may play a role to direct the assembly via templating. Overall, the results show that the combination of specific salts and enzymatic hydrogelation can give rise to complex self-assembly behaviors that may be exploited to tune hydrogel properties.

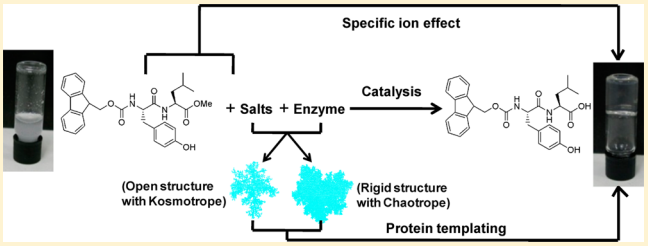

INTRODUCTION

Peptide-based functional nanomaterials have received extensive interest as next-generation materials for biomedicine as well as energy-related technologies.[1−21] A number of strategies have been developed to direct the molecular self-assembly of the peptide building blocks, such as changes in the environmental conditions, including pH, temperature, solvent polarity, ionic strength, oxidation/reduction state, etc.[22−30] An alternative approach is to use a locally applied stimulus, such as light[31,32] or catalytic action of the enzymes.[33,34] Enzymatic reactions are especially useful to direct bottom-up nanofabrication because they allow for directed self-assembly under otherwise constant conditions coupled with chemoselective and spatiotemporal control of nucleation and structure growth.[6,7]

Although the "specific ion" effect on protein folding and aggregation has been recognized since more than a century ago, in 1888, by Hofmeister,[35] the understanding of this effect still remains a source of controversy. Hofmeister classified the ions according to their relative ability of precipitating hen-egg white protein in aqueous solution, resulting in the sequence shown in Figure 1a. Two basic hypotheses have been put forward to account for this phenomenon.[36−41] One is attributed to the bulk effect, which involves the ability of the ions to make and break hydrogen bonds with water (kosmotropes and chaotropes, characterized by their Jones−Dole viscosity B coefficient, derived from the effects on viscosity).[42] The other hypothesis proposes a major role of dispersion forces. These specific ion effects have later been observed in other areas, such as colloid and surface chemistry, macromolecular systems, such as proteins and polymers, etc.[43−51] However, it has only recently been appreciated in supramolecular chemistry and, more specifically, for low-molecular-weight (LMW) hydrogels,[6,52−54] while a few reports have been published for polymer hydrogels.[55−58]

Very recently, we showed that salts can have a pronounced effect on molecular assembly and resulting material properties of a series of anionic Fmoc-peptide-based gelators, following the Hofmeister trend of anions.[52] Ions were found to have a significant influence on the hydrophobic interactions with minimal effect on hydrogen-bonding interactions, leading to more organized supramolecular structures for the kosmotropic ions compared to the chaotropic ions. This specific ion effect provides a powerful parameter that can control the formation of diverse nanostructures, accessible from a single gelator. Another recent example includes a macrocyclic LMW hydrogelator, proline-functionalized calix-[4]-arene, which showed ion-

Received: August 22, 2012
Revised: October 31, 2012
Published: November 1, 2012

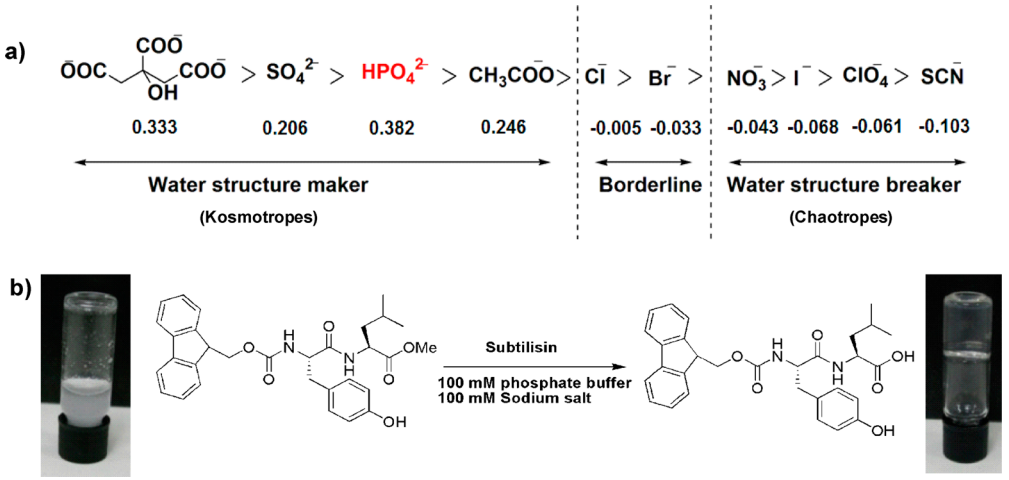

Figure 1. Biocatalytic self-assembly and gelation in the presence of salts. (a) Order of ions by their B coefficients. The placing of phosphates is debatable because of the presence of both $H_2PO_4^-$ and HPO_4^{2-} at near-neutral pH. (b) Subtilisin triggered hydrolysis of the Fmoc-YL-OMe to form hydrogelator Fmoc-YL.

specific sol–gel transition, but the effect of the salts on the molecular organization of the hydrogel was not studied.[53] Very recently, Adams et al. demonstrated a cation-specific effect on an anionic aromatic peptide gelator, where the electrostatic (cross-linking) interactions between the cation and gelator were shown to be important.[54]

Herein, we combine biocatalysis and molecular self-assembly in the presence of different salts to access diverse supramolecular nanostructures. We reveal a dual, cooperative effect of the salts on the molecular self-assembly of a Fmoc-dipeptide hydrogelator: (i) differential structuring of the enzyme molecules in the presence of different salts that affects the enzyme kinetics and may act as a template for self-assembly, in addition to the (ii) inherent salt effects on the self-assembly of the peptide hydrogelator. As might be expected, supramolecular order correlated with the presence of the kosmotropic salts compared to the chaotropic salts. Interestingly, we observed an unexpected effect on the handedness of the fibrillar structure with chiral inversion observed in the final gel-phase material.

RESULTS AND DISCUSSION

Biocatalytic Self-Assembly. The self-assembled system used in this study is based on an aromatic peptide amphiphile, Fmoc-tyrosine-leucine methyl ester (Fmoc-YL-OMe; Figure 1b).[52] Molecular self-assembly is induced by the hydrolysis of the methyl ester by an esterase, subtilisin, which cleaves the methyl ester to form the peptide derivative, Fmoc-YL, that self-assembles through a π-stacking interaction between the fluorenyl groups and finally interlocked into an antiparallel β-sheet structure, referred to as the π–β structure. The sodium salts given in Figure 1 were added at a concentration of 100 mM (Figure 1b). In each case, after 1 h of incubation at 55 °C, followed by cooling to room temperature (20 °C), self-supporting gels were formed. HPLC time courses revealed that the rate of biocatalysis was significantly affected by the presence of the salts and followed the relative ordering of the ions in Hofmeister series. Such an ion-specific effect on biocatalytic activity is well-known for a number of enzymes.[43−46] In each case, near-complete conversion was observed within 1 h (Figure 2), and therefore, final gelator concentrations were identical in each case. To ensure the complete conversion,

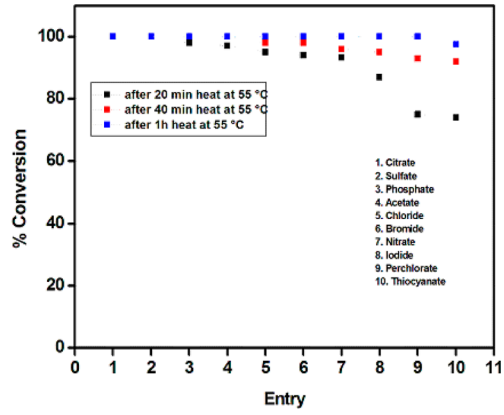

Figure 2. Time-dependent HPLC of the enzyme reaction with different salts.

further spectroscopic and structural analyses were performed after 24 h.

Self-assembly of these aromatic peptide amphiphiles is driven by noncovalent intermolecular interactions (π–π stacking, hydrogen-bonding interactions, etc.) in addition to the hydrophobic effect.[59−62] Such molecular level interactions can be followed by a number of spectroscopic methods. Our recent study on the dynamics of the self-assembly process has shown that molecular order was induced during enzyme conversion, driven by the hydrophobic effect and π-stacking interaction between the fluorenyl groups; it is locked into a β-sheet structure upon cooling.[6] Therefore, we will focus on the effects of the salts over supramolecular organization of fluorenyl groups.

Fluorescence emission spectra showed two characteristic peaks (Figure 3a) corresponding to the monomer and the highly π-stacked structure. The peak with a maximum at 320 nm corresponds to the monomeric Fmoc-YL emission, while the relatively broad peak at 420–440 nm is due to the excimer formation, owing to the π-stacking interactions between the fluorenyl groups. The intensity of the monomeric emission was found to be progressively quenched with respect to excimer emission in the expected order (chaotropes to kosmotropes). However, a red-shifted monomeric peak (340 nm) was observed for the Fmoc-YL gels in the presence of nitrate ion,

dx.doi.org/10.1021/la303388s | Langmuir 2012, 28, 16664−16670

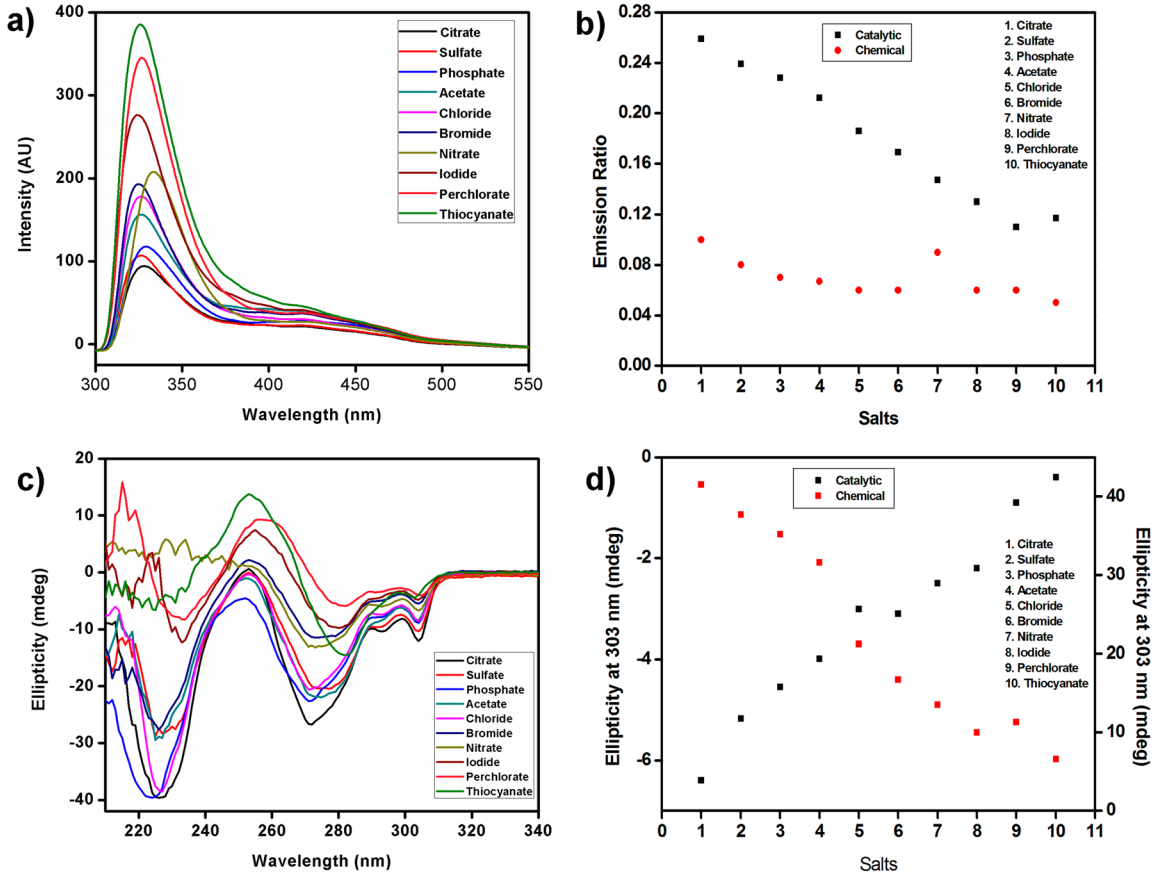

Figure 3. Spectroscopic evidence of induced supramolecular order in the presence of different salts for biocatalytic and chemical self-assembly. (a) Emission spectra (excitation at 280 nm) of Fmoc-YL gel obtained with different salt additives. (b) Emission ratio (ratio of intensity of the excimer to the monomer) for the biocatalytic and chemical self-assembly. (c) CD spectra of supramolecular hydrogel of Fmoc-YL, showing that higher order chirality is induced following the Hofmeister series. (d) Increase in the ellipticity at 303 nm from chaotropes to kosmotropes for the biocatalytic and chemical self-assembly.

suggesting a different supramolecular organization. The emission ratio, which is the relative intensity of the excimer to the monomer emissions, showed a higher value for the kosmotropes than chaotropes (Figure 3b), suggesting that kosmotropes promote the formation of extended $\pi-\pi$ interactions among the fluorenyl moieties and, thus, inducing more order in the self-assembled state. Importantly, the effects of salts were found to be significantly enhanced for biocatalytic self-assembly compared to the chemical self-assembly,[52] shown in Figure 3b.

It is well-known that the formation of supramolecular chiral structures gives rise to intense CD signals. Intense CD signals have been shown previously in Fmoc-dipeptide gels, and it originates principally from the supramolecular organization of the Fmoc substituent (in addition to contributions from the amide backbone and tyrosyl side chains).[59−62] CD spectra were recorded for Fmoc-YL gels in the presence of different salts, which showed a characteristic peak at 303 nm, corresponding to the fluorenyl absorption.[6] Figure 3c showed that all of these gels gave rise to a negative signal, which indicates the single handedness for the supramolecular structures. The extent of induced chirality, as shown in Figure 3d, was significantly affected by the salts; more intense CD was observed for kosmotropes compared to chaotropes. Surprisingly, we observed a chiral inversion in the enzyme-triggered self-assembly compared to the chemical self-assembly, as reported earlier.[52] We investigated whether these effects could be related to the kinetic effects of biocatalytic self-assembly and hydrogelation (Figure 2), as described in the next section. However, to assess whether the spectroscopic properties were affected by scattering, we have carried out the turbidity measurement (see Figure S1 of the Supporting Information), which showed the absence of significant interference from scattering.

To gain insight into the nanoscale morphological properties of the gels formed, atomic force microscopy was performed on Fmoc-YL gels produced in the presence of the sodium salts of phosphate (kosmotrope) and thiocyanate (chaotrope) (see Figure S2 of the Supporting Information). Remarkable morphological differences were observed. Gels formed in the presence of phosphate revealed a fibrous morphology, with dimensions ranging from 95 to 125 nm. In contrast, for thiocyanate less organized spherical aggregates were found to be formed of dimensions ranging from 150 to 600 nm. The formation of spherical aggregates rather than unidirectional fibers (see Figure S2a of the Supporting Information) for thiocyanate-containing gels (see Figure S2b of the Supporting Information) is in agreement with the corresponding reduction of the emission ratio and CD signal for thiocyanate.

Determination of the gel melting temperature also supported that the gels were structurally different. T_{gel} varies from 50 to 58 °C between the extreme chaotropes and kosmotropes (Figure 4a). The mechanical properties of these gels were then probed by oscillatory rheology. For all gels, the storage modulus (G')

dx.doi.org/10.1021/la303388s | *Langmuir* 2012, 28, 16664−16670

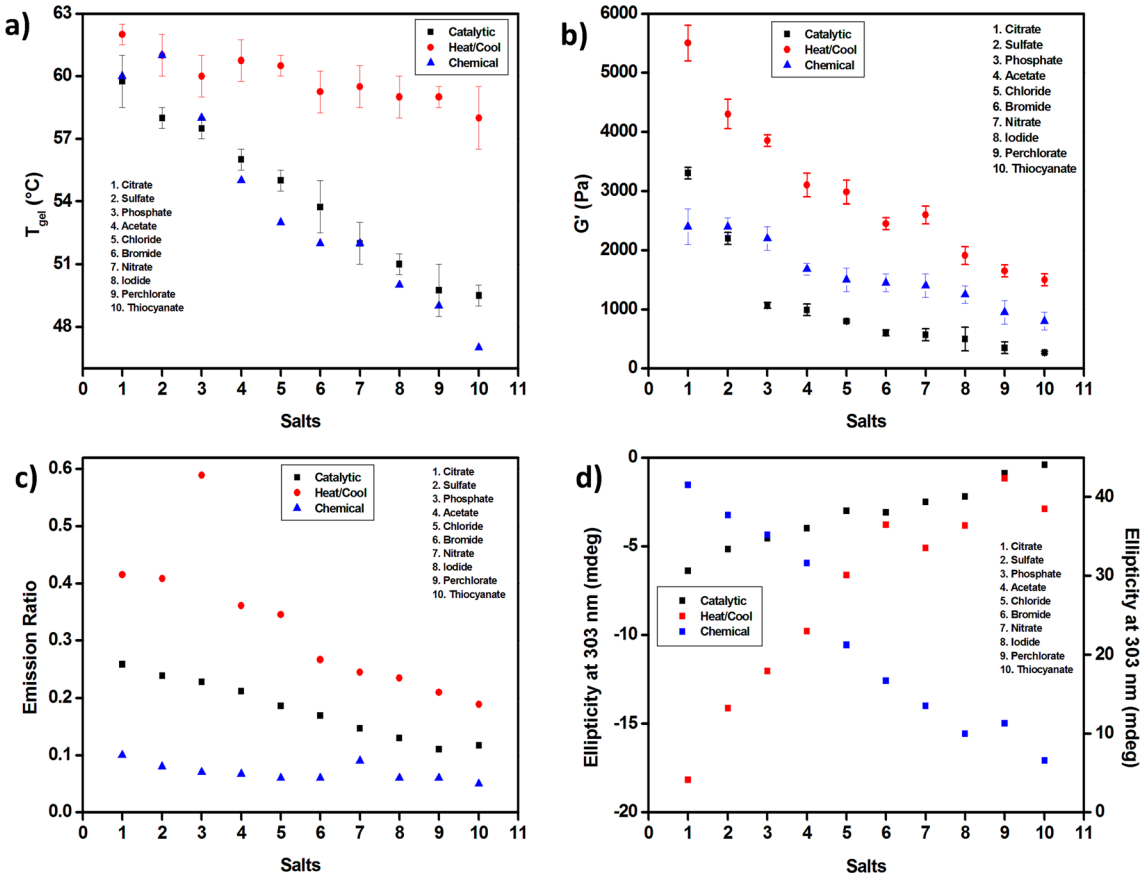

Figure 4. Thermal stability, mechanical strength, and spectroscopic behavior of the gels formed catalytically (black), by a heating–cooling cycle (red), and chemically (blue). (a) Melting temperature (T_{gel}) of Fmoc-YL gels formed in the presence of different salts. (b) Mechanical strength of Fmoc-YL gels with different salts as measured by oscillatory rheology. (c) Emission ratio (ratio of intensity of the excimer to the monomer) with different salts. (d) Increase in the ellipticity at 303 nm from chaotropes to kosmotropes.

was found to be an order of magnitude higher than the loss modulus (G''). G' varies from 0.3 to 3 KPa throughout the series (Figure 4b).

Thermodynamics versus Kinetics in Biocatalytic Assembly. After melting of the gels at 90 °C and cooling back to room temperature, all of the gels show a more pronounced salt-induced order in their self-assembled state, as reflected in their mechanical strength and induced supramolecular chirality (Figure 4 and Figure S3 of the Supporting Information). Although we did not find much difference in the thermal stability of the gels with different salts after the heat/cool cycle (Figure 4a), a pronounced effect was observed in the mechanical strength of the gels (Figure 4b), suggesting different self-assembled network structures. We also did not observe substantial differences in the emission ratio after heat/cool compared to the catalytic induction. An enhancement in the π-stacking interaction was observed, which reflected the enhanced salt-induced effect on the supramolecular chirality of the gels. A much higher emission ratio was again observed for phosphate ion, which is unexpected and will require further investigation. This observation indicates that, under catalytic control, kinetically trapped structures were formed, which access a more thermodynamically favored state upon heating/cooling. Salts, therefore, induced dual control of the biocatalytic self-assembly process as they influenced enzyme performance (affecting kinetics) as well as molecular level interactions between the gelator molecules and water molecules.

To investigate the possible templating effect of the enzyme, owing to their structuring/clustering in aqueous solution, as shown previously,[63,64] SLS was employed in the presence of different ions. The background-corrected SLS intensities are shown in Figure 5. The subtilisin molecules cluster to form

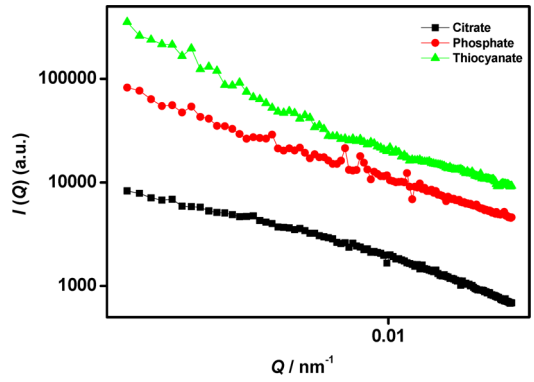

Figure 5. SLS intensities of subtilisin in the presence of different salts.

large aggregates at 55 °C, having a radius of gyration (R_g) of approximately 253 nm in the presence of kosmotropic salt, sodium citrate. The power law analysis used to characterize the fractal dimension exponent (d_f) of the clusters indicated the scattering pattern scales with an exponent of 1.5 in the Q region above 0.005 nm^{-1}, which indicates that the enzyme clusters

dx.doi.org/10.1021/la303388s | Langmuir 2012, 28, 16664–16670

form fairly open mass fractal structures in the presence of citrate ions (see Figure S4 of the Supporting Information). The power law exponent in the Q region below 0.005 nm^{-1} is around 1, suggesting that the subtilisin fractal clusters extend in one dimension to form structures similar to short rods. The scattering pattern of subtilisin in the presence of sodium phosphate resulted in a power law exponent of 1.6 in the whole range of scattering vector Q. It indicates that the fairly open mass fractal structures are present at all of the length scales. In contrast to the kosmotropic ions, the chaotropic thiocyante ion has different effects on the clustering of subtilisin molecules. The power law exponent changes from 1.6 (in the case of kosmotropic ions) to 2.5, which indicates the presence of dense mass fractal structures of enzymes, which are presumably rigid and less dynamic and may have buried active sites of enzyme in the presence of chaotropic thiocyanate ions (see Figure S4 of the Supporting Information).

These results suggest that the structuring of the subtilisin molecules plays an important role in the self-assembly of the Fmoc-YL hydrogelator. The kosmotropic ions favor the open and dynamic fractal networks of the enzymes, but the chaotropic ion generates a dense mass fractal structure. It is highly likely that these fractal structures also play a role as a template for self-assembly of the hydrogelator along with its enzymatic action.

■ CONCLUSION

We demonstrated that salts have a dramatic effect on the molecular self-assembly of the aromatic dipeptide amphiphiles in aqueous media. Salts affect the structuring of the enzyme network, which, in turn, influences the enzyme kinectics and the corresponding nucleation and growth of the nanostructures. This is manifested in the differential hydrophobic interactions, resulting in differential order and chirality as well as variable mechanical properties in the resulting gel-phase materials. The order of efficiency of the ions to promote such interactions followed the Hofmeister trend. Such a specific ion effect can be attributed to the complex interplay of both the electrostatic and hydrophobic interactions. Although the exact mechanism behind this effect is not fully understood, it can be rationalized by considering electrostatic screening of the charges, ion binding, and its implication to hydrophobic interactions, as discussed in our recent work.[52] The present study demonstrates that highly complex self-assembly behavior occurs when combining the effects of salts, protein templating, and catalysis. Insight into these behaviors is useful in controlling and directing peptide self-assembly toward desired nanomaterials.

■ EXPERIMENTAL SECTION

Catalytic Self-Assembly. Fmoc-YL-OMe (10 mmol/kg) was dispersed in a 1 mL volume of 100 mM sodium phosphate buffer (pH 8) in the presence of different sodium salts (100 mM) and 30 μL of subtilisin from Sigma-Aldrich (catalogue number P4860; LOT 056K1213) within a 10 mm sample vial. The mixture was vortexed (30 s) and sonicated on ice for 20 min to ensure that a homogeneous mixture was obtained, while the low temperature assures that no enzymatic conversion occurs up to this point. This was followed by heating in an oil bath at 55 °C for 60 min to allow for the enzymatic conversion to occur. The self-assembling system was then allowed to cool to room temperature. The gel samples were then left overnight before experimental measurements were performed. Gelation was considered to have occurred when a homogeneous "solid-like" material was obtained that exhibited no gravitational flow. The thermally reversible gel−sol transition temperature (T_{gel}) was determined using a vial inversion method at varying temperatures.

Fluorescence Spectroscopy. Fluorescence emission spectra were measured on a Jasco FP-6500 spectrofluorometer with light measured orthogonally to the excitation light, at a scanning speed of 100 nm min^{-1}. The excitation wavelength was 280 nm, and emission data were recorded in the range between 300 and 600 nm. The spectra were measured with a bandwidth of 5 nm with a medium response and a 1 nm data pitch. Quartz cells with a path length of 10 mm were used for the study.

Circular Dichroism (CD). Spectra were measured on a Jasco J600 spectropolarimeter with 1 s integrations with a step size of 1 nm and a single acquisition with a slit width of 1 nm because of the dynamic nature of the system. Quartz cells of 0.2 mm path length were used for the measurement.

High-Performance Liquid Chromatography (HPLC). A Dionex P680 HPLC pump was used to quantify conversions of the enzymatic reaction. A 50 μL sample was injected onto a Macherey-Nagel C18 column of 250 mm length with an internal diameter of 4.6 mm and 5 mm fused silica particles at a flow rate of 1 mL min^{-1} [eluting solvent system: linear gradient of 20% (v/v) acetonitrile in water for 4 min and gradually rising to 80% (v/v) acetonitrile in water at 35 min; this concentration was kept constant until 40 min when the gradient was decreased to 20% (v/v) acetonitrile in water at 42 min]. The sample preparation involved mixing 50 μL of gel with acetonitrile−water (950 μL, 50:50 mixture) containing 0.1% trifluoroacetic acid. The purity of each identified peak was determined by the ultraviolet (UV) detection at 280 nm.

Oscillatory Rheology. To verify the mechanical properties of the resulting hydrogels, dynamic frequency sweep experiments were carried out on a strain-controlled rheometer (Kinexus Pro rheometer) using parallel-plate geometry (20 mm diameter). The experiments were performed at 25 °C, and this temperature was controlled throughout the experiment using an integrated electrical heater. Additional precautions were taken to minimize solvent evaporation and to keep the sample hydrated: a solvent trap was used, and the internal atmosphere was kept saturated. To ensure that the measurements were made in the linear viscoelastic regime, an amplitude sweep was performed and the results showed no variation in elastic modulus (G') and viscous modulus (G'') up to a strain of 1%. The dynamic modulus of the hydrogel was measured as a frequency function, where the frequency sweeps were carried out between 0.1 and 100 Hz. The gels were made in small fractions in wide-mouth vials from which they were transferred with a spatula for rheological measurements. The measurements were repeated 3 times to ensure reproducibility, with the average data shown.

Static Light Scattering (SLS). SLS measurements were carried out using the 3DDLS instrument (LS Instruments, Fribourg, Switzerland) using vertically polarized He−Ne laser light (25 mW with a wavelength of 632.8 nm) with an avalanche photodiode detector at angles between 15° and 135° at 55 °C. The background scattering intensities (buffers with added salts) were subtracted from the scattering intensities of the enzyme solutions for further analysis. The scattering intensity patterns from static light and X-ray scattering experiments can be described as $I(Q) \sim KP(Q)S(Q)$, where K is an instrument- and sample-dependent constant, $P(Q)$ is the form factor that depends upon the size and shape of the primary particles, and $S(Q)$ is the structure factor giving information about the spatial arrangement of the primary particles at length scales larger than that of the primary particles (radius R_p). In the limit of $QR_g < 1$, the mean radius of gyration R_g of randomly distributed (e.g., freely diffusing) primary particles or clusters can be determined from the measured scattered intensity $I(Q)$ using the Guinier analysis. In the limit of $1/R_g \ll Q \ll 1/R_p$, where R_g is the mean radius of gyration of a sufficiently large cluster composed of primary particles with radius R_p, the structure factor for fractal clusters with fractal dimension d_f scales with Q through a power law relation as $I(Q) \sim S(Q) \sim Q^{-d_f}$. The radius of gyration can be calculated by plotting Q^2 and ln $I(Q)$, and then linear regression will give the slope, from where we can calculate R_g. The power law behavior and fractal dimension are calculated by plotting

the SLS data on a log−log scale and then performing a nonlinear fit, which provides a scaling factor called the fractal dimension.

■ ASSOCIATED CONTENT

Supporting Information

Turbidity data, AFM images of the gels with different salts. Fluorescence emission spectra of Fmoc-YL gels after the heat/cool cycle and open and rigid mass fractal structure of the enzyme in the presence of kosmotropic and chaotropic salts. This material is available free of charge via the Internet at http://pubs.acs.org.

■ AUTHOR INFORMATION

Corresponding Author

*E-mail: rein.ulijn@strath.ac.uk (R.V.U.); sangita.roy@strath.ac.uk (S.R.).

Notes

The authors declare no competing financial interest.

■ ACKNOWLEDGMENTS

We thank the EPSRC, HFSP, ERC (Starting Grant EMERgE), and Leverhulme Trust (Leadership Award) (U.K.) for funding. The material is based on research sponsored by the Air Force Laboratory, under Agreement FA9550-11-1-0263.

■ REFERENCES

(1) Estroff, L. A.; Hamilton, A. D. Water gelation by small organic molecule. *Chem. Rev.* **2004**, *104*, 1201.
(2) Lehn, J. M. *Supramolecular Chemistry—Concepts and Perspectives*; VCH: Weinheim, Germany, 1995.
(3) Reches, M.; Gazit, E. Casting metal nanowires within discrete self-assembled peptide nanotubes. *Science* **2003**, *300*, 625.
(4) Zhang, S. Fabrication of novel biomaterials through molecular self-assembly. *Nat. Biotechnol.* **2003**, *21*, 1171.
(5) Whitesides, G. M.; Grzybowski, B. A. Self-assembly at all scales. *Science* **2002**, *295*, 2418.
(6) Hirst, A. R.; Roy, S.; Arora, M.; Das, A. K.; Hodson, N.; Murray, P.; Marshall, S.; Javid, N.; Sefcik, J.; Boekhoven, J.; van Esch, J. H.; Santabarbara, S.; Ulijn, R. V. Biocatalytic induction of supramolecular order. *Nat. Chem.* **2010**, *2*, 1089.
(7) Williams, R. J.; Smith, A. M.; Collins, R. F.; Hodson, N.; Das, A. K.; Ulijn, R. V. Enzyme-assisted self-assembly under thermodynamic control. *Nat. Nanotechnol.* **2009**, *4*, 19.
(8) Yang, Z.; Liang, G.; Wang, L.; Xu, B. Using a kinase/phosphatase switch to regulate a supramolecular hydrogel and forming the supramolecular hydrogel in vivo. *J. Am. Chem. Soc.* **2006**, *128*, 3038.
(9) Yang, Z.; Gu, H.; Fu, D.; Gao, P.; Lam, J. K.; Xu, B. Enzymatic formation of supramolecular hydrogels. *Adv. Mater.* **2004**, *16*, 1440.
(10) Woolfson, D. N.; Ryadnov, M. G. Peptide-based fibrous biomaterials: Some things old, new and borrowed. *Curr. Opin. Chem. Biol.* **2006**, *10*, 559.
(11) Hartgerink, J. D.; Beniash, E.; Stupp, S. I. Peptide−amphiphile nanofibers: A versatile scaffold for the preparation of self-assembling materials. *Proc. Natl. Acad. Sci. U.S.A.* **2002**, *99*, 5133.
(12) Silva, G. A.; Czeisler, C.; Niece, K. L.; Beniash, E.; Harrington, D. A.; Kessler, J. A.; Stupp, S. I. Selective differentiation of neural progenitor cells by high-epitope density nanofibers. *Science* **2004**, *303*, 1352.
(13) De Loos, M. B. L. F.; van Esch, J. H. Design and application of self-assembled low molecular weight hydrogels. *Eur. J. Org. Chem.* **2005**, 3615.
(14) Van Esch, J. H. We can design molecular gelators, but do we understand them? *Langmuir* **2009**, *25*, 8392.
(15) Coates, I. A.; Smith, D. K. Hierarchical assembly—Dynamic gel−nanoparticle hybrid soft materials based on biologically derived building blocks. *J. Mater. Chem.* **2010**, *20*, 6696.
(16) Hamley, I. W. *Introduction to Soft Matter: Synthetic and Biological Self-Assembling Materials*; John Wiley and Sons: New York, 2007.
(17) Zhao, X. B.; Pan, F.; Xu, H.; Yaseen, M.; Shan, H. H.; Hauser, C. A. E.; Zhang, S. G.; Lu, J. R. Molecular self-assembly and applications of designer peptide amphiphiles. *Chem. Soc. Rev.* **2010**, *39*, 3480.
(18) Hamley, I. W. Self-assembly of amphiphilic peptides. *Soft Matter* **2011**, *7*, 4122.
(19) Ryan, D. M.; Doran, T. M.; Anderson, S. B.; Nilsson, B. L. Effect of C-terminal modification on the self-assembly and hydrogelation of fluorinated Fmoc-Phe derivatives. *Langmuir* **2011**, *27*, 4029.
(20) Debnath, S.; Shome, A.; Das, D.; Das, P. K. Hydrogelation through self-assembly of Fmoc-peptide functionalized cationic amphiphiles: Potent antibacterial agent. *J. Phys. Chem. B* **2010**, *114*, 4407.
(21) Cheng, G.; Castelletto, V.; Moulton, C. M.; Newby, G. E.; Hamley, I. W. Hydrogelation and self-assembly of Fmoc-tripeptides: Unexpected influence of sequence on self-assembled fibril structure, and hydrogel modulus and anisotropy. *Langmuir* **2010**, *26*, 4990.
(22) Smith, A. M.; Williams, R. J.; Tang, C.; Coppo, P.; Collins, R. F.; Turner, M. L.; Saiani, A.; Ulijn, R. V. Fmoc-diphenylalanine self assembles to a hydrogel via a novel architecture based on $\pi-\pi$ interlocked β-sheets. *Adv. Mater.* **2008**, *20*, 37.
(23) Jayawarna, V.; Ali, M.; Jowitt, T. A.; Miller, A. F.; Saiani, A.; Gough, J. E.; Ulijn, R. V. Nanostructured hydrogels for three-dimensional cell culture through self-assembly of fluorenylmethoxycarbonyl−dipeptides. *Adv. Mater.* **2006**, *18*, 611.
(24) Holmes, T. C.; de Lacalle, S.; Su, X.; Liu, G.; Rich, A.; Zhang, S. Extensive neurite outgrowth and active synapse formation on self-assembling peptide scaffold. *Proc. Natl. Acad. Sci. U.S.A.* **2000**, *97*, 6728.
(25) Jonkheijm, P.; van der Schoot, P.; Schenning, A. P. H. J.; Meijer, E. W. Probing the solvent-assisted nucleation pathway in chemical self-assembly. *Science* **2006**, *313*, 80.
(26) Fairman, R.; Åkerfeldt, K. S. Peptides as novel smart materials. *Curr. Opin. Struct. Biol.* **2005**, *15*, 453.
(27) Adams, D. J.; Frith, W. F.; Kirkland, M.; Mullen, L.; Sanderson, P. A new method for maintaining homogeneity during liquid−hydrogel transitions using low molecular weight hydrogelators. *Soft Matter* **2009**, *5*, 1856.
(28) Bowerman, C. J.; Nilsson., B. L. A reductive trigger for peptide self-assembly and hydrogelation. *J. Am. Chem. Soc.* **2010**, *132*, 9526.
(29) Hirst, A. R.; Coates, I. A.; Boucheteau, T.; Miravet, J. F.; Escuder, B.; Castelletto, V.; Hamley, I. W.; Smith, D. K. Low-molecular-weight gelators: Elucidating the principles of gelation based on gelator solubility and a cooperative self-assembly model. *J. Am. Chem. Soc.* **2008**, *130*, 9113.
(30) Rodriguez-Ilansola, F.; Miravet, J. F.; Escuder, B. Supramolecular gel formation and self-correction induced by aggregation-driven conformational changes. *Chem. Commun.* **2009**, 209.
(31) Haines, L. A.; Rajagopal, K.; Ozbas, B.; Salick, D. A.; Pochan, D. J.; Schneider, J. P. Light-activated hydrogel formation via the triggered folding and self-assembly of a designed peptide. *J. Am. Chem. Soc.* **2005**, *127*, 17025.
(32) Matsumoto, S.; Yamaguchi, S.; Ueno, S.; Komatsu, H.; Ikeda, M.; Ishizuka, K.; Iko, Y.; Tabata, K. V.; Aoki, H.; Ito, S.; Noji, H.; Hamachi, I. Photo gel−sol/sol−gel transition and its patterning of a supramolecular hydrogel as stimuli−responsive biomaterials. *Chem.—Eur. J.* **2008**, *14*, 3977.
(33) Yang, Z.; Liang, G.; Xu, B. Enzymatic hydrogelation of small molecules. *Acc. Chem. Res.* **2008**, *41*, 315.
(34) Ulijn, R. V. Enzyme-responsive materials: A new class of smart biomaterials. *J. Mater. Chem.* **2006**, *16*, 2217.
(35) Hofmeister, F. About the science of the effect of salts. *Arch. Exp. Pathol. Pharmakol.* **1888**, *24*, 247.
(36) Bauduin, P.; Renoncourt, A.; Touraud, D.; Kunz, W.; Ninham, B. W. Hofmeister effect on enzymatic catalysis and colloidal structures. *Curr. Opin. Colloid Interface Sci.* **2004**, *9*, 43.

(37) Kunz, W.; Lo Nostro, P.; Ninham, B. W. The present state of affairs with Hofmeister effects. *Curr. Opin. Colloid Interface Sci.* **2004**, *9*, 1.
(38) Hribar, B.; Southall, N. T.; Vlachy, V.; Dill, K. A. How ions affect the structure of water. *J. Am. Chem. Soc.* **2002**, *124*, 12302.
(39) Sachs, J. N.; Woolf, T. B. Understanding the Hofmeister effect in interactions between chaotropic anions and lipid bilayers: Molecular dynamics simulations. *J. Am. Chem. Soc.* **2003**, *125*, 8742.
(40) Gurau, M. C.; Lim, S.-M.; Castellana, E. T.; Albertorio, F.; Kataoka, S.; Cremer, P. S. On the mechanism of the Hofmeister effect. *J. Am. Chem. Soc.* **2004**, *126*, 10522.
(41) Paschek, D.; Ludwig, R. Specific ion effects on water structure and dynamics beyond the first hydration shell. *Angew. Chem., Int. Ed.* **2011**, *50*, 352.
(42) Jenkins, H. D. W.; Marcus, Y. Viscosity B-coefficients of ions in solution. *Chem. Rev.* **1995**, *95*, 2695.
(43) Yang, Z.; Liu, X.-J.; Chen, C.; Halling, P. J. Hofmeister effects on activity and stability of alkaline phosphatase. *Biochim. Biophys. Acta* **2010**, *1804*, 821.
(44) Collins, K. D. Ion hydration: Implications for cellular function, polyelectrolytes, and protein crystallization. *Biophys. Chem.* **2006**, *119*, 271.
(45) Salis, A.; Bilaničová, D.; Ninham, B. W.; Monduzzi, M. Hofmeister effects in enzymatic activity: Weak and strong electrolyte influences on the activity of *Candida rugosa* lipase. *J. Phys. Chem. B* **2007**, *111*, 1149.
(46) Pinna, M. C.; Salis, A.; Monduzzi, M.; Ninham, B. W. Hofmeister series: The hydrolytic activity of *Aspergillus niger* lipase depends on specific anion effects. *J. Phys. Chem. B* **2005**, *109*, 5406.
(47) Leontidis, E. Hofmeister anion effects on surfactant self-assembly and the formation of mesoporous solids. *Curr. Opin. Colloid Interface Sci.* **2002**, *7*, 81.
(48) Fedorov, M. V.; Goodman, J. M.; Schumm, S. To switch or not to switch: The effects of potassium and sodium ions on α-poly-L-glutamate conformations in aqueous solutions. *J. Am. Chem. Soc.* **2009**, *131*, 10854.
(49) Zhang, Y.; Cremer, P. S. Interactions between macromolecules and ions: The Hofmeister series. *Curr. Opin. Chem. Biol.* **2006**, *10*, 658.
(50) Batchelor, J. D.; Olteanu, A.; Tripathy, A.; Pielak, G. J. Impact of protein denaturants and stabilizers on water structure. *J. Am. Chem. Soc.* **2004**, *126*, 1958.
(51) Zhang, Y.; Furyk, S.; Bergbreiter, D. E.; Cremer., P. S. Specific ion effects on the water solubility of macromolecules: PNIPAM and the Hofmeister series. *J. Am. Chem. Soc.* **2005**, *127*, 14505.
(52) Roy, S.; Javid, N.; Frederix, P. W. J. M.; Lamprou, D. A.; Urquhart, A. J.; Hunt, N. T.; Halling, P. J.; Ulijn, R. V. Dramatic specific-ion effect in supramolecular hydrogels. *Chem.—Eur. J.* **2012**, *18*, 11723.
(53) Becker, T.; Goh, C. Y.; Jones, F.; Mclldowie, M. J.; Mocerino, M.; Ogden, M. I. Proline-functionalised calix[4]arene: An anion-triggered hydrogelator. *Chem. Commun.* **2008**, 3900.
(54) Chen, L.; Pont, G.; Morris, K.; Lotze, G.; Squires, A.; Serpell, L. C.; Adams, D. J. Salt-induced hydrogelation of functionalised-dipeptides at high pH. *Chem. Commun.* **2011**, *47*, 12071.
(55) Swann, J. M. G.; Bras, W.; Topham, P. D.; Howse, J. R.; Ryan, A. J. Effect of the Hofmeister anions upon the swelling of a self-assembled pH-responsive hydrogel. *Langmuir* **2010**, *26*, 10191.
(56) Xu, Y.; Wang, C.; Tam, K.; Li, L. Salt-assisted and salt-suppressed sol−gel transitions of methylcellulose in water. *Langmuir* **2004**, *20*, 646.
(57) Kundu, S. K.; Yoshida, M.; Shibayama, M. Effect of salt content on the rheological properties of hydrogel based on oligomeric electrolyte. *J. Phys. Chem. B* **2010**, *114*, 1541.
(58) Okazaki, Y.; Ishizuki, K.; Kawauchi, S.; Satoh, M.; Komiyama, J. Ion-specific swelling and deswelling behaviors of ampholytic polymer gels. *Macromolecules* **1996**, *29*, 8391.
(59) Tang, C.; Smith, A. M.; Collins, R. F.; Ulijn, R. V.; Saiani, A. Fmoc-diphenylalanine self-assembly mechanism induces apparent pK_a shifts. *Langmuir* **2009**, *25*, 9447.
(60) Chen, L.; Revel, S.; Morris, K.; Serpell, L. C.; Adams, D. J. Effect of molecular structure on the properties of naphthalene−dipeptide hydrogelators. *Langmuir* **2010**, *26*, 13466.
(61) Chen, L.; Morris, K.; Laybourn, A.; Elias, D.; Hicks, M. R.; Rodger, A.; Serpell, L. C.; Adams, D. J. Self-assembly mechanism for a naphthalene−dipeptide leading to hydrogelation. *Langmuir* **2010**, *26*, 5232.
(62) Gottarelli, G.; Lena, S.; Masiero, S.; Pieraccini, S.; Spada, G. P. The use of circular dichroism spectroscopy for studying the chiral molecular self-assembly: An overview. *Chirality* **2008**, *20*, 471.
(63) Javid, N.; Vogtt, K.; Roy, S.; Hirst, A. R.; Hoell, A.; Hamley, I. W.; Ulijn, R. V.; Sefcik, J. Supramolecular structures of enzyme clusters. *J. Phys. Chem. Lett.* **2011**, *2*, 1395−1399.
(64) Guilbaud, J. B.; Saiani, A. Using small angle scattering (SAS) to structurally characterise peptide and protein self-assembled materials. *Chem. Soc. Rev.* **2011**, *40*, 1200−1210.